*J. Fluid Mech.* (2013), *vol.* 737, *pp.* 329–348.  
doi:10.1017/jfm.2013.566

# On the $k_1^{-1}$ scaling in sink-flow turbulent boundary layers

**Shivsai Ajit Dixit**[1,2] **and O. N. Ramesh**[3,†]

[1]Indian Institute of Tropical Meteorology, Pashan, Pune 411008, India

[2]Department of Mechanical Engineering, Maharshi Karve Stree Shikshan Samstha's Cummins College of Engineering for Women, Karvenagar, Pune 411052, India

[3]Department of Aerospace Engineering, Indian Institute of Science, Bangalore 560012, India

(Received 21 September 2012; revised 9 July 2013; accepted 23 October 2013; first published online 25 November 2013)

Scaling of the streamwise velocity spectrum $\phi_{11}(k_1)$ in the so-called sink-flow turbulent boundary layer is investigated in this work. The present experiments show strong evidence for the $k_1^{-1}$ scaling i.e. $\phi_{11}(k_1) = A_1 U_\tau^2 k_1^{-1}$, where $k_1$ is the streamwise wavenumber and $U_\tau$ is the friction velocity. Interestingly, this $k_1^{-1}$ scaling is observed much farther from the wall and at much lower flow Reynolds number (both differing by almost an order of magnitude) than what the expectations from experiments on a zero-pressure-gradient turbulent boundary layer flow would suggest. Furthermore, the coefficient $A_1$ in the present sink-flow data is seen to be non-universal, i.e. $A_1$ varies with height from the wall; the scaling exponent $-1$ remains universal. Logarithmic variation of the so-called longitudinal structure function, which is the physical-space counterpart of spectral $k_1^{-1}$ scaling, is also seen to be non-universal, consistent with the non-universality of $A_1$. These observations are to be contrasted with the universal value of $A_1$ (along with the universal scaling exponent of $-1$) reported in the literature on zero-pressure-gradient turbulent boundary layers. Theoretical arguments based on dimensional analysis indicate that the presence of a streamwise pressure gradient in sink-flow turbulent boundary layers makes the coefficient $A_1$ non-universal while leaving the scaling exponent $-1$ unaffected. This effect of the pressure gradient on the streamwise spectra, as discussed in the present study (experiments as well as theory), is consistent with other recent studies in the literature that are focused on the structural aspects of turbulent boundary layer flows in pressure gradients (Harun *et al.*, *J. Fluid Mech.*, vol. 715, 2013, pp. 477–498); the present paper establishes the link between these two. The variability of $A_1$ accommodated in the present framework serves to clarify the ideas of universality of the $k_1^{-1}$ scaling.

**Key words:** boundary layer structure, turbulent boundary layers

† Email address for correspondence: onr@aero.iisc.ernet.in

## 1. Introduction

### 1.1. *Background*

The issue of the so-called $k_1^{-1}$ scaling has attracted a great deal of attention in the literature on turbulent boundary layers (TBLs) investigated in both the laboratory (Perry, Henbest & Chong 1986; Nickels *et al.* 2005) and the atmosphere (Katul & Chu 1998; Lauren *et al.* 1999; Högström, Hunt & Smedman 2002). In this paper, the $k_1^{-1}$ scaling in a special accelerating laboratory TBL flow, namely the sink-flow TBL, is examined; similar investigations for laboratory TBL flows have, so far, been limited to zero-pressure-gradient (ZPG) flows in the literature (Nickels *et al.* 2005). Strong experimental evidence for the occurrence of $k_1^{-1}$ scaling ($\phi_{11}(k_1) = A_1 U_\tau^2 k_1^{-1}$) in a relatively low-Reynolds-number sink-flow TBL will be presented. It will also be shown that although the scaling exponent in the observed sink-flow $k_1^{-1}$ variations is universal, the coefficient $A_1$ varies with the distance from the wall. This is to be contrasted with the universal value of $A_1$ reported in the literature for high-Reynolds-number (high-*Re*) ZPG TBL flows (Nickels *et al.* 2005).

The $k_1^{-1}$ scaling applies to those large-scale motions or eddies that: (i) contain a significant amount of the kinetic energy of turbulence (Perry *et al.* 1986); and (ii) possess friction velocity $U_\tau$, as the velocity scale over the entire range of their sizes (Davidson, Nickels & Krogstad 2006); $U_\tau = \sqrt{\tau_w/\rho}$ wherein $\tau_w$ is the wall-shear stress and $\rho$ is the density of fluid. For such motions if there exists sufficient spectral overlap between motions that scale on the inner flow variables and those which scale on the outer flow variables then it can be shown that the power spectral density (PSD) $\phi_{11}(k_1)$ of streamwise velocity fluctuation $u$, in the spectral overlap zone, must vary inversely with the streamwise wavenumber $k_1$, i.e. $\phi_{11}(k_1) \propto k_1^{-1}$. Inner scaling uses $y$ and $U_\tau$ as the length and velocity scales for turbulent motions whereas outer scaling uses $\delta$ and $U_\tau$ for the same (Perry *et al.* 1986). Here $y$ is the wall-normal distance and $\delta$ is the boundary-layer thickness.

It has been shown that for the $k_1^{-1}$ scaling of the streamwise spectrum, one necessary condition is that the kinetic energy of the contributing eddies scales on $U_\tau^2$ (Davidson *et al.* 2006; Davidson & Krogstad 2009). If this is true, then this raises a question of whether the superstructure-type motions (Hutchins & Marusic 2007*b*) could, by themselves, contribute to the $k_1^{-1}$ scaling in ZPG TBL flows. This is so because it is known that although the spatial extent of superstructures scales on the outer length scale $\delta$, the superstructure energy (especially the low-wavenumber hump in the premultiplied streamwise spectra for a high-*Re* ZPG TBL flow) does not simply scale on $U_\tau$ (Hutchins & Marusic 2007*b*). Furthermore, Nikora (1999) has noted that the presence of coherent structures is not essential for the $k_1^{-1}$ scaling. This is further discussed in § 3.1 in some detail.

The PSD $\phi_{11}(k_1)$ of $u$ is defined (see Perry *et al.* 1986) by the relation

$$\overline{u^2} = \int_0^\infty \phi_{11}(k_1)\,\mathrm{d}k_1, \tag{1.1}$$

where the overbar denotes time-average. The $k_1^{-1}$ scaling, in the spectral overlap zone, is given by

$$\frac{k_1\phi_{11}}{U_\tau^2} = A_1, \tag{1.2}$$

where the coefficient $A_1$ is independent of $k_1$.

There are a variety of ways in which the $k_1^{-1}$ scaling may be derived (Perry *et al.* 1986; Sreenivasan 1989; Nikora 1999; Davidson *et al.* 2006). The most widely used approach is the spectral scaling and spectral overlap arguments that use dimensional analysis (Perry *et al.* 1986; Nickels *et al.* 2005); the theory presented in § 4 of the present paper uses this approach.

### 1.2. *Attached motions in a ZPG flow and a sink flow*

It has been emphasized that for observing the $k_1^{-1}$ scaling, measurements must be made very close to the wall in a high-$Re$ flow (Nickels *et al.* 2005). Here we assess these requirements in the context of sink-flow TBLs using the so-called attached-eddy model and by making comparison with the existing ZPG data. While the attached-eddy framework is used as a conceptual template in the present work to bring out aspects related to sink-flow TBLs in relation to the corresponding ZPG flows, it must be remembered that this is only one of the many alternatives. For example, Davidson & Krogstad (2009) have proposed an analytical model for TBL flows that does not predicate upon the existence of attached eddies. In addition, it has already been suggested that the superstructures may not contribute to the $k_1^{-1}$ scaling directly (§ 1.1) and this further makes the simple arguments presented below particularly relevant.

It is known that the attached-eddy model leads to: (i) the $k_1^{-1}$ scaling of the streamwise spectrum; and (ii) the pure-wall flow with logarithmic mean velocity profile (Perry & Chong 1982; Perry & Marusic 1995); throughout this paper *pure-wall flow* means the TBL flow wherein the wake component of the structure does not exist, i.e. the wake factor is zero. This implies that one should have a wide range of *attached* motions for the $k_1^{-1}$ scaling to become evident (Nickels *et al.* 2007). For ZPG TBL flows, Perry & Marusic (1995) have shown that extra eddies (type-B eddies) that do not extend physically to the wall (i.e. detached eddies) are required in the model in addition to the original attached eddies (type-A eddies) of Perry & Chong (1982); the $k_1^{-1}$ scaling is however contributed to only by the attached eddies. Further, it is important to note that only part of the entire range of attached eddy sizes in effect contributes to the $k_1^{-1}$ scaling of the spectrum. We shall call these the $k_1^{-1}$ eddies. Nickels *et al.* (2007) have noted that the size of the largest attached eddy contributing to the $k_1^{-1}$ range (i.e. the largest $k_1^{-1}$ eddy) in a ZPG flow is of the order of $0.1\delta$ and this corresponds to the height from the wall where the mean-velocity log law region ends. Note that the changeover from log law to wake profile in a ZPG flow is smooth and therefore it is difficult to ascertain the corresponding wall-normal location exactly; the estimates for the end of mean velocity log law range from $y = 0.1\delta$ to $0.2\delta$ (Marusic *et al.* 2013).

Consider first the ZPG flow of Nickels *et al.* (2005) having Reynolds number $\delta_+ = \delta U_\tau/\nu = 14\,380$; here $\nu$ is kinematic viscosity of the fluid. For this flow, the $k_1^{-1}$ range, spanning over 30 % of a decade in $k_1$, is observed around $y/\delta = 0.008$ ($y_+ \approx 100$). Let the height, corresponding to the size of the largest $k_1^{-1}$ eddy in a ZPG flow, be $\delta_1$ ($\delta_1 \approx 0.1\delta$). The Reynolds number $\delta_{1+}$, based on thickness of this region, would then be $\delta_{1+} \approx 0.1\delta_+ = 1438$. Let the height of the measurement location be $\delta_2$ ($\delta_2 = 0.008\delta$). Hence, the ratio of largest to smallest attached scales contributing to the $k_1^{-1}$ scaling in the high-$Re$ ZPG flow of Nickels *et al.* (2005) is $\delta_1/\delta_2 \approx 0.1/0.008 = 12.5$.

Consider now the sink-flow TBL which develops downstream in a self-similar fashion under a favourable pressure gradient (FPG). In this paper, *sink-flow TBL* means a TBL flow that has *reached* the asymptotic state (zero wake factor) while developing in the sink-flow FPG. It is known that such flow: (i) is a pure-wall flow

| TBL flow | Size $\delta_1$ of the largest $k_1^{-1}$ eddy | Scale separation $\delta_1/\delta_2$ of the $k_1^{-1}$ eddies | $y_+$ at $\delta_2$ | $y/\delta$ where $k_1^{-1}$ scaling is expected to emerge | Reynolds number $\delta_+$ |
|---|---|---|---|---|---|
| ZPG flow | $\sim 0.1\delta$ | 10 | $\sim 100$ | $\sim 0.01$ | $\sim 10\,000$ |
| Sink flow | $\sim\delta$ | 10 | $\sim 100$ | $\sim 0.1$ | $\sim 1000$ |

TABLE 1. Expectations from a ZPG flow and a sink-flow TBL based on a decade of scale separation of the $k_1^{-1}$ eddies. Here $\delta_2$ is the height of the measurement location from the wall. The beginning of the mean-velocity log law region is assumed to be $y_+ \sim 100$ for simplicity.

with the mean-velocity log law starting next to the buffer layer and extending almost all through the boundary layer up to its mean edge (Jones, Marusic & Perry 2001; Dixit & Ramesh 2008); and (ii) can be modelled by considering attached eddies (type-A eddies) alone (Perry & Marusic 1995). Therefore, the size $\delta_1$ of the largest $k_1^{-1}$ eddy in a sink-flow TBL may be expected to be of order $\delta$ itself, i.e. $\delta_1 \approx \delta$ (and, hence, $\delta_{1+} \approx \delta_+$). This is to be contrasted with the ZPG flow where $\delta_1 \approx 0.1\delta$ as mentioned earlier. In other words, based on the Reynolds number of the largest $k_1^{-1}$ eddy, a sink-flow TBL with $\delta_+ = 1438$ may be considered to be equivalent (in a limited sense) to a ZPG flow with $\delta_+ = 14\,380$. Whether such an equivalence extends to other aspects of these flows (structural details, for instance) is an interesting question but that is beyond the scope of the present paper. It follows that for the same scale separation $\delta_1/\delta_2 \approx 12.5$ as in the ZPG case, one has to have $\delta_2 \approx (1/12.5)\delta = 0.08\delta$ in the sink-flow TBL. This value is an order of magnitude larger than $\delta_2 = 0.008\delta$ in the ZPG flow discussed in the previous paragraph. Note that the beginning of the log law region is assumed to be about $y_+ \sim 100$ in both cases; the main conclusion however remains unchanged by the specific choice of $y_+$. It is interesting to note that the sink-flow experiments by Jones (1998) show evidence in support of the above arguments; figure 5.13 therein shows that for $\delta_+$ values ranging from 723 to 1757, there is indeed a substantial $k_1^{-1}$ range at $y/\delta = 0.11$; see also appendix A in this connection. Table 1 summarizes the expectations from a ZPG flow and a sink-flow TBL based on the above discussion as referenced to a decade of scale separation of the $k_1^{-1}$ eddies.

The main difference between a high-*Re* ZPG TBL and the corresponding low-Reynolds-number (low-*Re*) sink-flow TBL is thus the manner in which comparable scale separation for $k_1^{-1}$ eddies is achieved. In ZPG flows, the upper bound of the range of $k_1^{-1}$ eddy sizes is fixed at $y \sim 0.1\delta$ and therefore the lower bound has to be pushed further down the range by increasing the flow Reynolds number (i.e. small-scales becoming smaller); in addition there is a certain indirect influence of the low-wavenumber hump which is discussed in some detail in § 3.1. In sink-flow TBLs, however, the upper bound itself moves out to $y \sim \delta$ (i.e. large scales becoming larger) and therefore large-scale separation for $k_1^{-1}$ eddies is obtained at a relatively lower Reynolds number and at locations not extremely close (in terms of $y/\delta$) to the wall.

Thus, the sink-flow TBLs could be an attractive framework for investigating the $k_1^{-1}$ scaling at: (i) Reynolds number $\delta_+$ which is almost an order of magnitude lower; and (ii) a wall-normal distance $y/\delta$ which is almost an order of magnitude larger, than that required by the corresponding ZPG flow. Furthermore, one expects the large-scale structures in a sink-flow TBL to be of larger streamwise extent than those in a ZPG

flow at the same Reynolds number (Dixit & Ramesh 2010). This may render the $k_1^{-1}$ scaling observable over a larger extent in the spectral space compared with that in a ZPG flow.

The present paper is organized in the following fashion. In § 2 experimental details of the sink-flow set-up are presented. Section 3 presents streamwise velocity spectra for a sink-flow TBL in addition to the longitudinal structure function data which is the physical-space counterpart of streamwise spectra. Section 4 presents theoretical arguments that support the remarkable features of the sink-flow spectra of § 3. Section 5 presents conclusions.

## 2. Sink-flow TBL experiments

Pitot-tube and hotwire-anemometry measurements of sink-flow TBLs with varying pressure gradients and Reynolds numbers have been carried out in a suction-type open-circuit wind tunnel facility (test-section cross-section of 1 foot × 1 foot) at the Department of Aerospace Engineering, Indian Institute of Science, Bangalore, India. The facility has been described in detail in Dixit & Ramesh (2008, 2010) (henceforth DR08 and DR10). For the present study of streamwise velocity spectra in a sink-flow TBL configuration, raw data from the experiments of DR08 and DR10 has been used.

The flow PG1 of DR10, having $\delta_+ = 803$ and $\Delta_p = -0.0086$, is being considered here since this is the highest-Reynolds-number sink-flow TBL studied therein. Here $\Delta_p = (\nu/\rho U_\tau^3)\,\mathrm{d}p/\mathrm{d}x$ is the wall-scaled dimensionless pressure gradient. Each $u$ signal has been sampled at $f_s = 10$ kHz (sample interval $\Delta t = 1/f_s = 1 \times 10^{-4}$ s) for $T = 61.44$ s using a single-wire probe. At the measurement station L4 (see DR08), $\delta = 14.1$ mm, $U_\tau = 0.8545$ m s$^{-1}$ and the free-stream velocity $U_\infty = 19.2$ m s$^{-1}$ giving $\delta_+ = 803$, $\Delta_p = -0.0086$ and $C_f = 2(U_\tau/U_\infty)^2 = 0.00396$. The acceleration parameter is $K = (\nu/U_\infty^2)\,\mathrm{d}U_\infty/\mathrm{d}x = 7.58 \times 10^{-7}$. Dimensionless sampling parameters are $\Delta t_+ = \Delta t U_\tau^2/\nu = 4.87$ and $TU_\infty/\delta = 83\,663$. Note that $\Delta t_+ = 4.87$ is only marginally larger than the recommended value of ∼3 and the consequent temporal resolution error is expected to be relatively insignificant (see figure 16 from Hutchins *et al.* 2009). The non-dimensional sensor length $l_+$ is 45 and the length-to-diameter ratio $l/d$ is approximately 160.

## 3. Experimental results and their discussion

### 3.1. *Streamwise velocity spectra*

In the present work, the wavelet transform has been used to obtain the PSD of streamwise velocity fluctuation by: (i) splitting the parent $u$ signal into 24 equal parts (duration of each part being approximately $83\,663/24 = 3486$ boundary-layer turnover times); (ii) obtaining the PSD for each part by employing the complex-Morlet wavelet transform (Uddin, Perry & Marusic 1997) using MATLAB; and (iii) ensemble-averaging all 24 PSDs to form the final spectrum. It has been verified that the wavelet spectrum so obtained faithfully follows the fast Fourier transform (FFT) spectrum and is much smoother than the latter. Frequency-to-wavenumber conversion is carried out by Taylor's frozen-turbulence hypothesis ($k_1 = 2\pi f_1/U_c$) with the use of local mean velocity $U$ as the convection velocity $U_c$.

Figure 1 shows premultiplied spectra in outer and inner scalings. Wall-normal locations used in figure 1 are required to be free of any substantial viscous effects since the $k_1^{-1}$ scaling is considered to be an inviscid expectation (see § 4); this issue is discussed in some detail at the end of this subsection. The most striking feature of figure 1 is the presence of a prominent $k_1^{-1}$ variation seen as a plateau in each

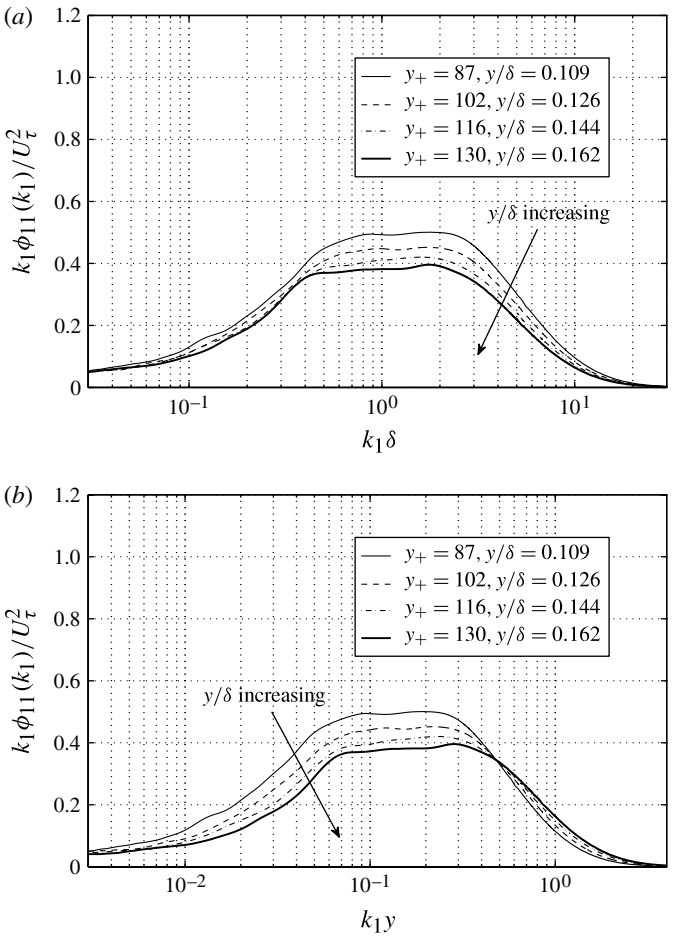


FIGURE 1. Premultiplied streamwise velocity spectra (using wavelets) for the present sink-flow TBL (flow PG1 in DR10; $\delta_+ = 803$ and $\Delta_p = -0.0086$): (*a*) outer scaling and (*b*) inner scaling.

spectrum for the wall-normal locations $87 \leqslant y_+ \leqslant 130$; outside this range of wall-normal locations (not shown) no $k_1^{-1}$ variation is observed. Note that each plateau extends over the same range of wavenumbers in both scalings confirming genuine spectral overlap. Typical extent of the $k_1^{-1}$ variation, at $y_+ = 87$, is $\sim$29 % of a decade in $k_1$ ($0.8 \leqslant k_1\delta \leqslant 2.3$ in figure 1*a*) which is indeed substantial. In the case of ZPG flow of Nickels *et al.* (2005), a similar extent ($\sim$30 % of a decade in $k_1$) is observed at a much higher Reynolds number $\delta_+ = 14\,380$. Also note that the $k_1^{-1}$ range in figure 1 emerges at $y/\delta = 0.109$, a distance which is substantially farther from the wall compared with that in a ZPG flow. These observations are consistent with the arguments of § 1.2 and corresponding expectations outlined in table 1.

Figure 1(*a*) shows that the spectra showing the $k_1^{-1}$ range exhibit reasonable collapse in the outer scaling (to within the experimental uncertainty of $\pm 3$ %) towards the low-wavenumber end ($k_1\delta < 0.3$). However, spectra in inner scaling do not collapse (figure 1*b*) but in fact exhibit a systematic shift with a crossover around $k_1y = 0.5$. Also, it is interesting to note that the $k_1^{-1}$ plateaus of figure 1 do not collapse onto

one another but instead exhibit a systematic shift. This indicates that while the scaling exponent $-1$ is universal, the coefficient $A_1$ is not; $A_1$ varies with the distance from the wall. As will be shown later, the variation of $A_1$ values in figure 1 is $\sim$24 % which is well outside the typical measurement uncertainty of $\pm 3$ %. This is to be contrasted with the high-*Re* ZPG TBL flows where a universal value for $A_1$ has been observed (Nickels *et al.* 2005). The lack of universality of $k_1^{-1}$ variations in sink-flow TBLs has been cursorily noted by Jones (1998). Table 2 presents a summary of the experimental data on ZPG and sink-flow TBLs (see also § 1.2 and table 1 for comparison).

By $k_1^{-1}$ scaling what is usually meant is that the spectra (1.2) measured at different heights in the flow should *collapse* onto a single horizontal line over a range of wavenumbers in both inner as well as outer scalings (Nickels *et al.* 2005). However, the present experimental data suggests that the existence of $k_1^{-1}$ variation of $\phi_{11}$ at a particular height from the wall and the collapse of such variations from different heights could well be distinct issues. This is discussed from the viewpoint of spectral scaling arguments in § 4.

An interesting connection can be made between the present findings and the argument presented by Sreenivasan (1989) towards the $k_1^{-1}$ scaling. For a ZPG flow at sufficiently high Reynolds number, Sreenivasan (1989) argues that the dependence of the near-wall spectrum on $y$ must vanish in the constant-stress region since not much distinguishes one layer from another (a local-interaction approximation); this yields the universal $k_1^{-1}$ scaling. It is known that for TBL flows in strong pressure gradients, the constant-stress layer ceases to exist (Townsend 1976). However, one may view the near-wall region as a stack of subregions where each subregion is sufficiently thin for the variation of stress to be negligible. Now one may apply the arguments of Sreenivasan (1989) in a piecewise fashion, to all of the subregions and this would yield $k_1^{-1}$ scaling with a non-universal coefficient $A_1$.

Note that there is no hump at low wavenumbers in the sink-flow spectra of figure 1. This feature appears to be intrinsic to all of the available sink-flow data irrespective of Reynolds number (see Jones 1998) as will be shown in appendix A; this suggests that the absence of hump in sink-flow data is not merely a low-*Re* effect. In moderate- and high-*Re* ZPG flows on the other hand, there exists a low-wavenumber hump at $k_1\delta \approx 2$ in the near-wall spectra (figure 2 of Nickels *et al.* 2005) and is considered to be contributed to by the superstructures residing in the log region (Hutchins & Marusic 2007*b*). It is known that in TBL flows, the streamwise FPG attenuates large-scale energy and makes the superstructures less energetic (Harun *et al.* 2013). Thus, the generic absence of hump in sink-flow TBLs appears to be an FPG effect. The wavelengths ($\lambda_1 = 2\pi/k_1$) contributing to the $k_1^{-1}$ plateau in figure 1 typically range from $3\delta \leqslant \lambda_1 \leqslant 10\delta$. The corresponding range in the high-*Re* sink-flow TBL of Jones (1998) (see appendix A) is $0.8\delta \leqslant \lambda_1 \leqslant 10\delta$. These wavelengths are much longer compared with the wavelengths $0.125\delta \leqslant \lambda_1 \leqslant 0.314\delta$ that contribute to the $k_1^{-1}$ scaling in a high-*Re* ZPG flow (see figure 3 of Nickels *et al.* 2005); note that the wavelengths in the ZPG case are much shorter than the typical streamwise extent of the superstructures ($\geqslant 6\delta$, see Hutchins & Marusic 2007*b*) in line with our contention that the superstructures are unlikely to contribute to the $k_1^{-1}$ scaling directly in ZPG TBL flows (see § 1.1). The presence of long wavelengths contributing to the plateaus of figure 1 suggests however that the superstructures, although weakened by the FPG, may be contributing to the $k_1^{-1}$ scaling in sink-flow TBLs. Interestingly, this suggests that the superstructure energy in sink flows may scale simply on $U_\tau^2$. This aspect however requires further investigations in sink-flow TBLs. With this, one may now understand the indirect effect of the low-wavenumber hump on the $k_1^{-1}$ scaling. In the

https://doi.org/10.1017/jfm.2013.566 Published online by Cambridge University Press





| Flow | Size $\delta_1$ of largest $k_1^{-1}$ eddy | $y/\delta = \delta_2/\delta$ where $k_1^{-1}$ scaling is seen to emerge | Scale separation $\delta_2/\delta_1$ of $k_1^{-1}$ eddies | Extent of the $k_1^{-1}$ scaling as % of a decade in $k_1$ | Universality of the coefficient $A_1$ |
|---|---|---|---|---|---|
| ZPG flow of NMHC ($\delta_+ = 14\,380$) | $\sim 0.1\delta$ | $\sim 0.008$ | 12.5 | $\sim 30$ | Universal $A_1 =$ constant |
| ZPG flow of HM[a] ($\delta_+ = 7271$) | $\sim 0.1\delta$ | $\sim 0.012$ | 8.33 | $\sim 10$ | Universal $A_1 =$ constant |
| Sink flow of MJ ($\delta_+ = 1756$) | $\sim \delta$ | $\sim 0.05$ | 20 | $\sim 100$ | Non-universal $A_1 = A_1(y/\delta)$ |
| Sink flow PG1 of DR10 ($\delta_+ = 803$) | $\sim \delta$ | $\sim 0.109$ | 9.17 | $\sim 30$ | Non-universal $A_1 = A_1(y/\delta)$ |

TABLE 2. Experimental data of ZPG and sink-flow TBLs with reference to the $k_1^{-1}$ scaling. NMHC, Nickels *et al.* (2005); HM, Hutchins & Marusic (2007*a*); MJ, Jones (1998); and DR10, Dixit & Ramesh (2010). [a] Denotes datasets from the original authors reanalysed here but not shown in this paper.

case of a ZPG flow, it is conceivable that with the increase in Reynolds number, the $k_1^{-1}$ plateau tends to form and grow to the high-wavenumber end. But, simultaneously, the low-wavenumber hump also grows due to strengthening of superstructures and encroaches on the plateau from the low-wavenumber side (Hutchins & Marusic 2007*b*); this possibly offsets the gain in the width of the plateau. One therefore needs to reach very high Reynolds numbers before observing a reasonable $k_1^{-1}$ plateau. In the case of sink-flow TBLs however, FPG suppresses the outer site and hence the hump, making the $k_1^{-1}$ plateau evident at much lower Reynolds numbers.

Before closing this section, we assess the effects of viscosity for the wall-normal locations of figure 1. It has been suggested that the $k_1^{-1}$ region in boundary layers is expected to occur around $y_+ \approx 100$ (Nickels *et al.* 2007), i.e. where the widest range of contributing attached motions exists without strong viscous effects. This corresponds to the approximate beginning of the logarithmic region in the mean velocity description. However, the current understanding of ZPG TBLs, channels and pipes prescribes $y_+ = 2.6(\delta_+)^{1/2}$ as the Reynolds-number-dependent outer limit of the viscosity-dominated near-wall region (Wei *et al.* 2005; Marusic *et al.* 2013). Borrowing this estimate for the present sink-flow case yields $y_+ > 74$ for neglecting the viscous effects. Another estimate, which is more relevant in FPG situations such as the present one, comes from the study of Metzger, Lyons & Fife (2008). They find, based on the mean momentum balance measurements in a TBL flow in sink-flow FPG, that the viscous effects extend out to the location where the Reynolds shear stress reaches its maximum. This location, denoted by $y_{peak+}$, is observed to vary with the Reynolds number according to $y_{peak+} = 4.2(\delta_+)^{1/3}$ which is the equation of the dashed line in figure 21(*b*) of Metzger *et al.* (2008). This estimate yields $y_+ > 39$ for the viscous effects to be negligible in the present sink-flow TBL. The approximate beginning of the mean velocity logarithmic region for the present sink flow (see DR08 and DR10) is $y_+ \approx 70$ which is not inconsistent with the above estimates. Furthermore, one may use the estimates of Reynolds number $R_{\lambda_T} = \lambda_T\sqrt{\overline{u^2}}/\nu$ based on the Taylor microscale $\lambda_T$ and the root-mean-square (r.m.s.) velocity fluctuation $\sqrt{\overline{u^2}}$ in this connection (see Nickels *et al.* 2007). Nickels *et al.* use $R_{\lambda_T} \geqslant 100$ as a sufficient condition to argue that the viscous effects for their data are negligible. The present sink-flow data show that $R_{\lambda_T}$ is in fact of the order of 200 for the wall-normal locations of figure 1; here $\lambda_T$ is estimated from $\phi_{11}(k_1)$. In addition, as will be shown in the next subsection, the streamwise intensity follows logarithmic variation, an inviscid expectation arising from the attached-eddy hypothesis, beyond $y/\delta = 0.12$ which is consistent with the emerging $k_1^{-1}$ region around the same wall-normal location. The above discussion shows that the wall-normal locations of figure 1 are well outside the mean-flow viscous effects. Similarly one may demonstrate that the wavelengths contributing to the $k_1^{-1}$ plateaus of figure 1 are more than 10 times the corresponding Taylor microscales implying that the $k_1^{-1}$ scaling is indeed contributed by the inviscid motions.

### 3.2. *Wall-normal variation of streamwise intensity*

Figure 2(*a*) shows the measured variation of streamwise intensity across the present sink flow TBL. Measurements have been corrected for the spatial resolution error ($l_+ = 45$ for this flow) using the scheme of Smits *et al.* (2011). This yields the error in the normalized intensity to be only $\sim$6 % of the measured value at $y_+ = 87$ and 4 % at $y_+ = 130$. This is therefore not of much concern in the present context of the $k_1^{-1}$ scaling. It is clear that for $0.12 \leqslant y/\delta \leqslant 0.72$, the variation of intensity

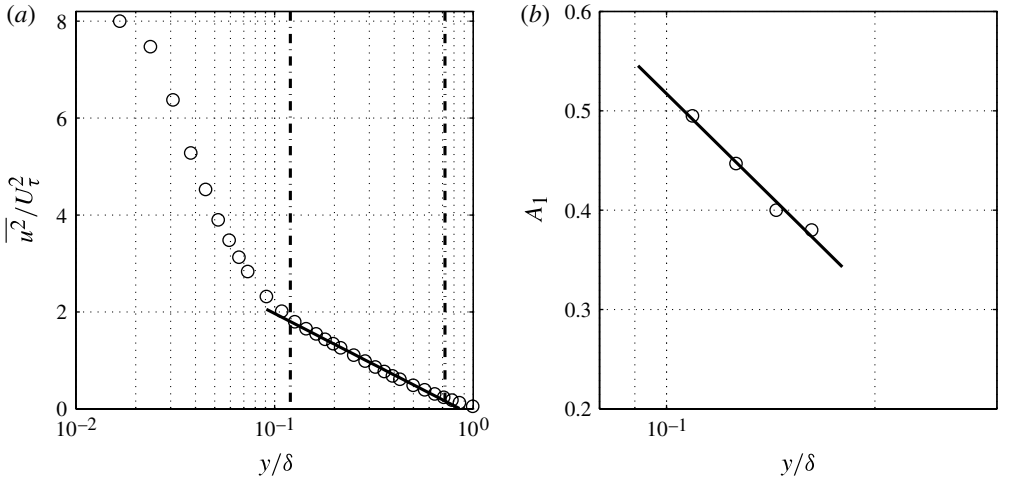


FIGURE 2. (*a*) Streamwise turbulence intensity profile corrected for spatial resolution error ($l_+ = 45$ for this flow) using the scheme of Smits *et al.* (2011) and (*b*) variation of the coefficient $A_1$ in (1.2) with $y/\delta$ for spectra of figure 1, in the case of the present sink-flow TBL (flow PG1 in DR10; $\delta_+ = 803$ and $\Delta_p = -0.0086$). Solid lines are logarithmic fits to the corresponding data. Vertical dashed-dotted lines in (*a*) indicate the extent of the logarithmic fit.

is logarithmic consistent with the predictions of the attached-eddy model (Townsend 1976; Perry & Marusic 1995; Nickels *et al.* 2007); this supports the expectation further that the sink-flow TBL is populated by only the attached eddies (§ 1.2). Simple geometrical arguments for the shape of spectra ($87 \leqslant y_+ \leqslant 130$) of figure 1(*a*) indicate that the functional form for the variation of coefficient $A_1$ with height from the wall may be expected to be the same as that for the intensity. In order to see this, note that: (i) each spectrum of figure 1(*a*) encloses an area below it that resembles a trapezium, the total area being equal to the normalized intensity at that height from the wall; and (ii) equal areas under the curve represent equal contributions to the intensity. Further, each trapezium may be imagined to be made up of the central rectangle under the plateau and the two triangles on its either side. It may be observed that as one moves outwards from the wall, the major contribution to the change in area under the spectral curve comes from the change in height $A_1$ of the central rectangle; the width of the rectangle remains fairly unaltered. Thus, $A_1$ may be expected to be proportional to the streamwise intensity for $87 \leqslant y_+ \leqslant 130$ (i.e. $0.109 \leqslant y/\delta \leqslant 0.162$) in figure 1(*a*). Figure 2(*b*) shows that over this range of wall-normal locations, $A_1$ indeed varies logarithmically with $y/\delta$.

Comparison with the ZPG data at matched $\delta_+$ indicates that the drop of intensity in a sink flow, with distance from the wall, is more rapid than in a ZPG flow (see appendix B). This appears to be due to the weakening of the outer energy site because of the FPG (see Harun *et al.* 2013) which causes significant spatial transport of the turbulence kinetic energy (TKE) as compared with the ZPG flow. Thus, in a sink-flow TBL, the rapid drop of intensity is related to the wall-normal variation of $A_1$ through spatial transport of TKE. There is however significant spectral transfer of energy as well and this is exemplified by significant values (of the order of 200) of the Taylor-microscale Reynolds number discussed before in § 3.1. Furthermore, this connection between the $A_1$ value and the streamwise intensity appears to be crucial

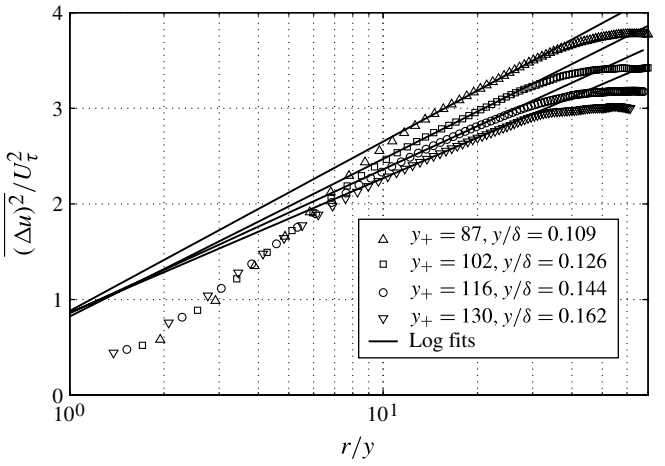


FIGURE 3. Normalized longitudinal structure function plotted against dimensionless streamwise separation for the present sink-flow TBL (flow PG1 in DR10; $\delta_+ = 803$ and $\Delta_p = -0.0086$). Wall-normal locations as in figure 1. Solid lines indicate logarithmic fits as per (3.2).

to understanding the commonly conceived notion of spectral *collapse* of $k_1^{-1}$ variations (i.e. a universal value for $A_1$) in ZPG flows. Indeed for such flows, the intensity is almost invariant with the height from the wall (plateau in the intensity profile implying negligible spatial transport of the TKE) over the range of wall-normal locations where a universal value for $A_1$ is observed (see Nickels *et al.* 2007).

### 3.3. *Longitudinal structure function*

The authenticity of non-universal $A_1$ values for the $k_1^{-1}$ scaling observed in figure 1 may be evaluated by making use of the so-called longitudinal structure function $\overline{(\Delta u)^2}(r)$ which is the spatial counterpart of $\phi_{11}(k_1)$ (Davidson *et al.* 2006).

The longitudinal structure function $\overline{(\Delta u)^2}(r)$ is, by definition,

$$\overline{(\Delta u)^2}(r) = \overline{(u(x) - u(x+r))^2} = 2\overline{u^2}(1 - f(r)), \tag{3.1}$$

where $r$ is the streamwise spatial separation between the two measurement locations lying in the same spanwise and wall-normal plane.

Davidson *et al.* (2006) have shown that the physical-space equivalent of the spectral $k_1^{-1}$ scaling is the logarithmic variation of $\overline{(\Delta u)^2}(r)$ given by

$$\overline{(\Delta u)^2}(r) = U_\tau^2[A + B\ln(r/y)]. \tag{3.2}$$

For ZPG flows, Davidson *et al.* (2006) have found the values of parameters $A$ and $B$ in (3.2) to be universal and equal to 2.04 and 1.83, respectively.

Figure 3 shows the variations of $\overline{(\Delta u)^2}(r)$ in the present sink flow TBL for the four wall-normal locations of interest (see figure 1). Here $\overline{(\Delta u)^2}(r)$ is calculated directly by delaying the time-series of $u$ and converting the time delay $\Delta t$ into spatial distance $r$ using Taylor's hypothesis $r = -U_c\Delta t$. Local mean velocity $U$ is used as the convection velocity $U_c$ (DR10; Davidson *et al.* 2006). It is clear that each structure function curve shows a definite region of logarithmic variation implying existence of

the spectral $k_1^{-1}$ scaling. However these logarithmic variations show systematic changes in slope $B$ (intercept $A$ in (3.2) is almost unaltered) with the height from the wall. This yields strong support for the observed non-universality of coefficient $A_1$ in the $k_1^{-1}$ scaling of figure 1.

## 4. Scaling of the streamwise velocity spectra in TBL flows

Results of § 3 prompt an enquiry into the scaling arguments for streamwise spectra in smooth-wall-bounded TBL flows. In particular, we would like to assess the issue of universality of the exponent in the $k_1^{-1}$ scaling along with the concomitant non-universality of the coefficient $A_1$. Towards this, we consider the outer and inner scaling of $\phi_{11}$ respectively as

$$\phi_{11} = f_1(\delta, U_\tau, k_1, \rho, \mathrm{d}p/\mathrm{d}x), \tag{4.1}$$

$$\phi_{11} = f_2(y, U_\tau, k_1, \rho, \mathrm{d}p/\mathrm{d}x). \tag{4.2}$$

Here $\mathrm{d}p/\mathrm{d}x$ is the streamwise pressure gradient as measured at the solid wall which equals the free-stream pressure gradient $\mathrm{d}p_\infty/\mathrm{d}x$ under the boundary-layer approximation. The present analysis pertains to large eddies of the flow and therefore fluid viscosity $\nu$ does not enter the analysis explicitly. Inclusion of $\mathrm{d}p/\mathrm{d}x$ in (4.1) and (4.2) is the main difference between the present scaling arguments and those to date (Perry *et al.* 1986; Nickels *et al.* 2005). Recent experimental studies on TBL flows with pressure gradients indicate that the large-scale structures in the flow indeed respond systematically to the applied pressure gradient (DR10; Harun *et al.* 2013).

Dimensional analysis of (4.1) and (4.2) yields the respective premultiplied spectra

$$\frac{k_1\phi_{11}}{U_\tau^2} = F_1(k_1\delta, \Pi_\delta), \tag{4.3}$$

$$\frac{k_1\phi_{11}}{U_\tau^2} = F_2(k_1 y, \Pi_y). \tag{4.4}$$

Here $\Pi_\delta = (\delta/\rho U_\tau^2)\,\mathrm{d}p/\mathrm{d}x = \delta_+\Delta_p$ and $\Pi_y = (y/\rho U_\tau^2)\,\mathrm{d}p/\mathrm{d}x = y_+\Delta_p$ are outer- and inner-scaled measures of the pressure gradient; observe that $\Pi_y = (y/\delta)\Pi_\delta$. Note that $\Pi_\delta$ is the ratio of average streamwise pressure force on the entire TBL flow to the average shear force at the wall (per unit width of the flow). Similarly $\Pi_y$ is the ratio of average streamwise pressure force up to height $y$ to the average shear force at the wall (per unit width of the flow). At a given streamwise station of measurement, $\Pi_\delta$ is a constant and therefore (4.3) and (4.4) yield

$$\frac{k_1\phi_{11}}{U_\tau^2} = F_1(k_1\delta)|_{\Pi_\delta}, \tag{4.5}$$

$$\frac{k_1\phi_{11}}{U_\tau^2} = F_2(k_1 y, y/\delta)|_{\Pi_\delta}. \tag{4.6}$$

Equation (4.5) implies collapse of outer-scaled spectra measured at different heights from the wall. On the other hand, (4.6) suggests the *lack* of collapse of inner-scaled spectra measured at different heights due to the presence of $y/\delta$. Note that (4.6) resembles (35) from Perry *et al.* (1986).

At this point it is important to make a comparison of the present theory, developed so far, with the model of TBL flow proposed by Davidson & Krogstad (2009). This model incorporates the low-*Re* effects for a ZPG TBL flow by accommodating a

correction term involving the ratio of production $P$ to dissipation $\epsilon$. In moderate- or low-*Re* ZPG flows, where production is not equal to dissipation, this term becomes important; the inner scaling inherits the effect of outer length scale due to this term and the inner scaling becomes 'mixed' (see § IIC of Davidson & Krogstad 2009). This bears strong resemblance to the arguments presented above wherein a similar effect of variation of $P/\epsilon$ is likely to be at work, not so much because of the low Reynolds number but mainly because of the FPG. Also the constant $B$ in Davidson & Krogstad's model ($B$ is proportional to $A_1$ in the present work) is a function of the Kármán constant $\kappa$ (a coefficient, to be precise). It has already been shown (DR08) that $\kappa$ could become a non-universal function of pressure gradient. In view of this, it is possible to derive support for the present premise of non-universal $k_1^{-1}$ scaling from the Davidson & Krogstad model also. Thus, the present theory seems to accommodate such detailed aspects in a simple fashion.

Continuing with the present analysis, we observe that in the case of TBL flows with pressure gradients, the outer scaling (4.5) is parameter-free but the inner scaling (4.6) is of parametric form, $y/\delta$ being the parameter. For the spectrum measured at a given height $y/\delta$ from the wall, right-hand side of (4.6) is simply $F_2(k_1y)|_{\Pi_\delta,y/\delta}$ and then spectral overlap between (4.5) and (4.6) requires

$$F_1(k_1\delta)|_{\Pi_\delta} = F_2(k_1y)|_{\Pi_\delta,y/\delta} = A_1(y/\delta)|_{\Pi_\delta}. \tag{4.7}$$

Note that the coefficient $A_1(y/\delta)|_{\Pi_\delta}$ is independent of $k_1$, but depends on the wall-normal location of measurement in a given flow. Thus in the spectral overlap zone of TBL flows with pressure gradients, we have

$$\frac{k_1\phi_{11}}{U_\tau^2} = A_1(y/\delta)|_{\Pi_\delta}, \tag{4.8}$$

which indicates a universal scaling exponent of $-1$, i.e. a $k_1^{-1}$ scaling, however, with a non-universal coefficient $A_1$ that depends on the wall-normal location of measurement. Results of § 3.2 indicate that the functional form of $A_1(y/\delta)$ in the present sink-flow TBL is logarithmic, i.e. $A_1 = a\ln(y/\delta) + b$, where $a$ and $b$ are constants for a given flow.

To summarize, the inner-scaled streamwise spectra (4.6) acquire parametric form (dimensionless distance from the wall being the parameter) on account of the existence of mean streamwise pressure gradient and thus fail to collapse in inner scaling ($0.08 \leqslant k_1y \leqslant 1$ in figure 1*b*). The outer-scaled spectra (4.5) however remain parameter-free ($k_1\delta < 2.3$ in figure 1*a*) and hence exhibit collapse in outer scaling ($k_1\delta < 0.4$ in figure 1*a*). The overlap of these spectral descriptions, in the form of a $k_1^{-1}$ scaling (4.8), inherits parametric form from the parent inner scaling. This explains the observed non-universality ($y/\delta$ dependence) of the spectral coefficient $A_1$ (the shift of plateaus in figure 1) in the present sink-flow data. Note that ZPG flow is a special (degenerate) case of the present scaling arguments wherein we trivially have $\Pi_\delta = 0$ as $\mathrm{d}p/\mathrm{d}x = 0$. Owing to this, the parametric form of inner scaling (4.6) vanishes, leading to a universal value of the coefficient $A_1$ in the $k_1^{-1}$ scaling for high-*Re* ZPG flows.

## 5. Conclusions

The present study investigates, experimentally and theoretically, the $k_1^{-1}$ scaling in sink-flow TBLs. It is found that a substantial $k_1^{-1}$ scaling range ($\sim$30 % of a decade in $k_1$) becomes apparent in the present experimental sink-flow data at much lower Reynolds number and much farther from the wall in comparison with the ZPG TBL

flows reported in the literature. Further, the coefficient $A_1$ in the $k_1^{-1}$ scaling is found to be non-universal for the present sink-flow TBL. Results for the longitudinal structure function offer further support for these observations. The non-universality of $A_1$ in the present sink-flow $k_1^{-1}$ scaling is to be contrasted with the universal value reported for $A_1$ in the literature on high-*Re* ZPG flows. Scaling arguments based on dimensional analysis suggest that the streamwise pressure gradient does not affect the exponent $-1$ in the spectral scaling but renders the coefficient $A_1$ non-universal, i.e. $A_1$ varies with the height from the wall. The universality of $A_1$ in high-*Re* TBL flows is a natural consequence of the present theory; in that sense the present work clarifies ideas of universality of the $k_1^{-1}$ scaling.

Streamwise turbulence intensity is found to exhibit logarithmic variation over large part of the present sink-flow TBL. The rapid drop of intensity with the distance from the wall in a sink-flow TBL, as compared with a ZPG flow at matched $\delta_+$, results in non-universal values of the spectral coefficient $A_1$. The structural reason for this appears to be the FPG-induced weakening of the superstructures and, hence, the outer energy site in sink-flow TBLs.

## Acknowledgements

We would like to record our thanks to (the late) Dr T. Nickels for useful discussions and suggestions. Thanks are also due to Dr M. Jones for providing the time-series data of his sink-flow TBL measurements and to Dr N. Hutchins and Professor I. Marusic for providing their experimental spectral data on ZPG flows. We would also like to thank Mr S. Patwardhan for providing the low-*Re* ZPG data from his experiments.

## Appendix A. Low-*Re* effects on the $k_1^{-1}$ scaling in sink-flow TBLs

In this appendix, we present the high-*Re* sink-flow spectral data of Jones (1998). We also examine the low-*Re* effects and estimate the lowest limiting sink-flow Reynolds number for observing a discernible $k_1^{-1}$ scaling range.

Figure 4 shows the spectra at different wall-normal locations in the sink-flow TBL of Jones having $\delta_+ = 1756$. Although this flow has not quite reached the asymptotic sink-flow state (see appendix B), it exhibits all the essential spectral features that are required to demonstrate the unique character of sink-flow TBLs. Raw voltage signals have been reprocessed to generate the spectra shown in figure 4(*a*,*b*); a Savitzky–Golay filter has been used to smooth the spectra. All of the interesting features, elaborated in § 3 in the context of the present sink flow, are exhibited by these spectra as well. These features include: (i) the collapse of spectra for low wavenumbers in the outer scaling; (ii) the lack of collapse (with a cross-over) in the inner scaling; (iii) the shifting of plateau levels with $y/\delta$; (iv) the presence of long wavelengths (up to $10\delta$ in figure 4) contributing to the $k_1^{-1}$ scaling range; and (v) the absence of the low-wavenumber hump. The most striking feature of figure 4 is the existence of $k_1^{-1}$ scaling over a full decade of scale separation. As mentioned before, the lack of universality of the $k_1^{-1}$ scaling alluded to in §§ 3.1 and 3.2 was cursorily noted by Jones (1998) also.

To examine the low-*Re* effects, we consider two more sink-flow TBLs from the study of DR08 having $\delta_+ = 525$ and 664, respectively, in addition to the present sink-flow TBL having $\delta_+ = 803$ and the sink flow of Jones (1998) having $\delta_+ = 1756$. These flows respectively have $\Delta_p = -0.0129$, $-0.0104$, $-0.0086$ and $-0.0033$. Therefore, $\Pi_\delta = \delta_+ \Delta_p$ values for these flows are $-6.7725$, $-6.9056$, $-6.8972$ and $-5.7948$, respectively, which are reasonably close to each other (to within 16 %). The last value

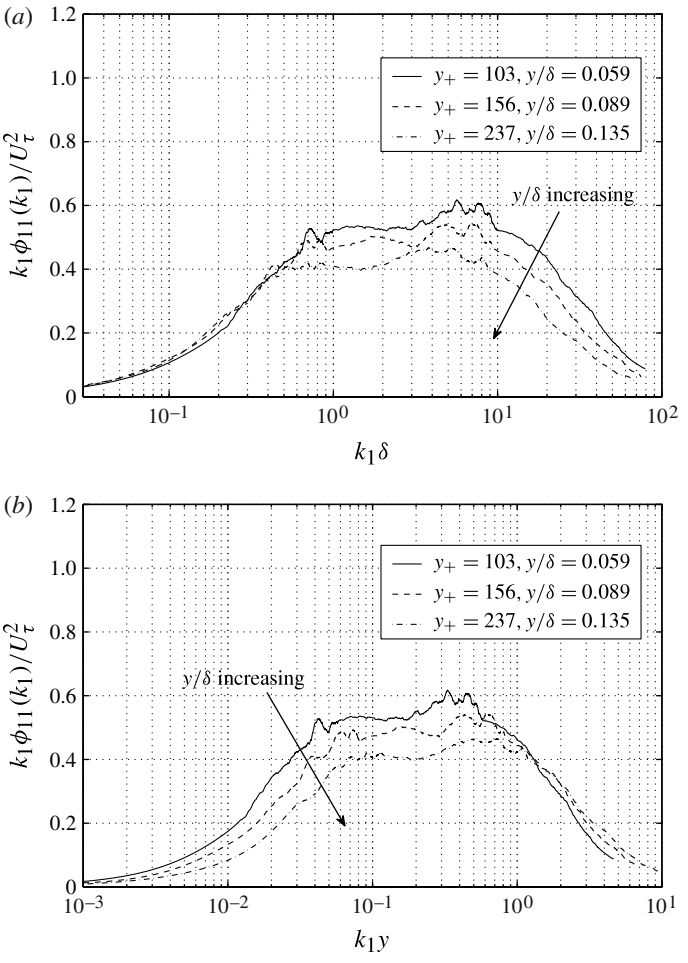


FIGURE 4. Premultiplied streamwise spectra for the sink-flow TBL of Jones (1998). For this flow $\delta_+ = 1756$, $K = 2.7 \times 10^{-7}$ and $\Delta_p = -0.0033$. (*a*) Outer scaling and (*b*) inner scaling. Alternate wall-normal locations are shown to avoid clutter and clarify the shift of plateaus.

is slightly lower compared with the remaining values which could either be a genuine trend or it could be due to the fact that the flow of Jones (1998) is somewhat away from the asymptotic sink-flow state. However, for the present discussion, this variation in $\Pi_\delta$ can be neglected since it does not affect the results of this appendix in a major way. The theory presented in § 4 indicates that the spectral coefficient $A_1$ in the $k_1^{-1}$ scaling is a function of $y/\delta$ provided that $\Pi_\delta = \text{constant}$. Given this, one may plot the spectra at matched $y/\delta$ (see (4.8)) across different sink flows as shown in figure 5.

Figure 5 shows that as the Reynolds number is increased from $\delta_+ = 525$ to 803, the $k_1^{-1}$ plateau appears at $\delta_+ = 803$. For lower Reynolds numbers, there is hardly any plateau in the spectrum (although there is an increasing tendency towards it) indicating the absence of $k_1^{-1}$ scaling due to insufficient attached scale separation. Note that the peak value of the pre-multiplied PSD and the area under the curve, which is the broadband inner-scaled streamwise intensity, both reduce with this initial increase of Reynolds number without appreciable broadening of the spectral width;

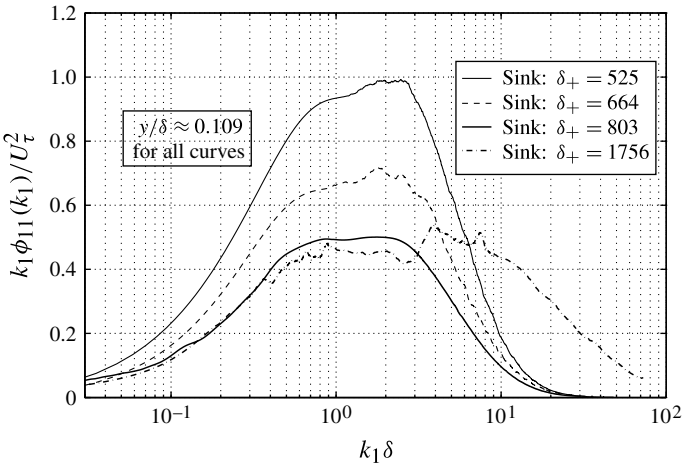


FIGURE 5. Low-Reynolds-number effects in the sink-flow streamwise spectra. Comparison of spectra with different Reynolds numbers at matched $y/\delta = 0.109$. Spectra for $\delta_+ = 525$, 664 and 1756 are smoothed by applying Savitzky–Golay filter to the FFT spectra. The spectrum for $\delta_+ = 803$ is from figure 1.

the peak transforms progressively into a plateau due to growing proportion of the low-wavenumber energy. However, following the appearance of the $k_1^{-1}$ plateau at $\delta_+ = 803$, further increase in Reynolds number thereon results in: (i) extension of the $k_1^{-1}$ plateau to higher wavenumbers without appreciable change in the value of $A_1$ (consistent with (4.8)); and (ii) collapse of spectra at low wavenumbers (consistent with (4.5)). From these observations, it is apparent that the minimum sink-flow TBL Reynolds number $\delta_+$ showing a discernible $k_1^{-1}$ scaling range lies between 664 and 803.

In § 3.2, it was argued that the variation of spectral coefficient $A_1$ with $y/\delta$ in a given sink flow ($\Pi_\delta = \text{constant}$) is expected to be logarithmic, i.e. $A_1 = a\ln(y/\delta) + b$. Equation (4.8), on the other hand, indicates that in general $A_1 = A_1(y/\delta, \Pi_\delta)$. It is therefore reasonable to expect that the parameters $a$ and $b$ in the logarithmic variation of $A_1$ would be functions of $\Pi_\delta$, i.e. $A_1(y/\delta, \Pi_\delta) = a(\Pi_\delta)\ln(y/\delta) + b(\Pi_\delta)$. Figure 6 shows variations of $A_1$ in the wall-normal direction for two sink-flow TBLs; $A_1$ values for the flow of Jones are taken from figure 4 and those for the present sink flow are taken from figure 2(*b*). Figure 6 demonstrates that $A_1$ indeed varies logarithmically in both the sink flows and the parameters of this variation are could well be functions of $\Pi_\delta$ as discussed before. Figure 6 indicates that the rate of variation of $A_1$ with $y/\delta$, i.e. slope $a(\Pi_\delta)$ decreases as the Reynolds number is increased. This is consistent with the expectation of a universal value for $A_1$ in the limit of infinite Reynolds number (see § 5). More data on sink-flow TBLs, covering a wide range of Reynolds numbers, is however required to confirm this observation.

## Appendix B. Pressure-gradient effect and the logarithmic intensity distribution in sink-flow TBLs

Figure 2(*a*) shows that the drop of intensity in the present sink-flow TBL is indeed logarithmic over $0.12 \leqslant y/\delta \leqslant 0.72$. The purpose of this appendix is to demonstrate that the drop of intensity in sink-flow TBL is more rapid as compared with a ZPG

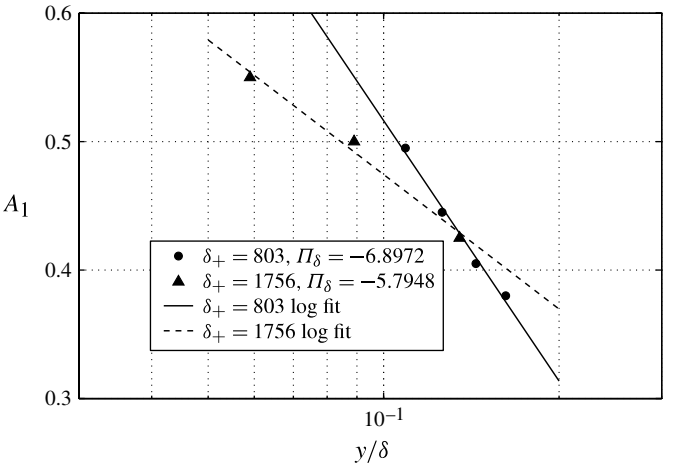


FIGURE 6. Logarithmic variation of the spectral coefficient $A_1$ (see (4.8)) in sink-flow TBLs at two different Reynolds numbers. Each thick line is a fit to the corresponding data according to $A_1 = a \ln(y/\delta) + b$.

TBL at matched Reynolds number $\delta_+$ and this is distinctively an FPG effect and not a low-*Re* effect. Towards this the experimental results of Harun *et al.* (2013) are important. This study investigates ZPG, FPG and APG layers at matched $\delta_+$. Figure 2(*b*) from Harun *et al.* clearly shows that in the case of FPG flow, the plateau or bump in the intensity distribution is suppressed and the intensity drop is steeper than in the ZPG flow at matched $\delta_+$. Note that the suppression of intensity bump leads to a tendency towards logarithmic variation of intensity as the pressure gradient is made favourable. This is true despite the fact that the FPG layer of Harun *et al.* is not a precise sink-flow layer and has much milder FPG than the present sink flow. This indicates that, at matched $\delta_+$, the steep drop of intensity due to the suppression of the bump is a pressure-gradient effect. The structural reason for this is considered to be FPG-induced weakening of the superstructures and hence the outer energy site in the TBL flow (Harun *et al.* 2013).

To illustrate this point in the present sink-flow case, consider figure 7 which shows the wall-normal distribution of the streamwise intensity for the present sink flow ($\delta_+ = 803$) compared with the ZPG intensity distributions at three different Reynolds numbers ($\delta_+ = 614$, 1014 and 1163). Note that the $\delta_+$ values of 614 and 1014 for the ZPG flow are on either side of the sink flow $\delta_+$ value of 803. With Reynolds number, the ZPG distributions exhibit systematic growth of the intensity bump in the neighbourhood of $y_+ = 200$. The intensity profile for a ZPG flow with $\delta_+ = 803$ must therefore lie between the profiles for $\delta_+ = 614$ and 1014. Such a profile however would be markedly different from the sink-flow profile, i.e. at matched $\delta_+ = 803$. This illustrates dramatic effect of FPG in making the outer site less energetic and causing the intensity to drop steeply (logarithmically in the sink-flow case, to be precise). An appeal to the TKE equation would suggest that the suppressed outer site is consistent with enhanced spatial transport of the TKE from the inner to the outer site and this appears to be responsible for the wall-normal variation in the value of the spectral coefficient $A_1$ (see § 3.2).

It is also instructive to appeal to the high-*Re* sink-flow data of Jones (1998) in the present context. Figure 8 shows the sink-flow intensity profiles with $\delta_+ = 1092$ and

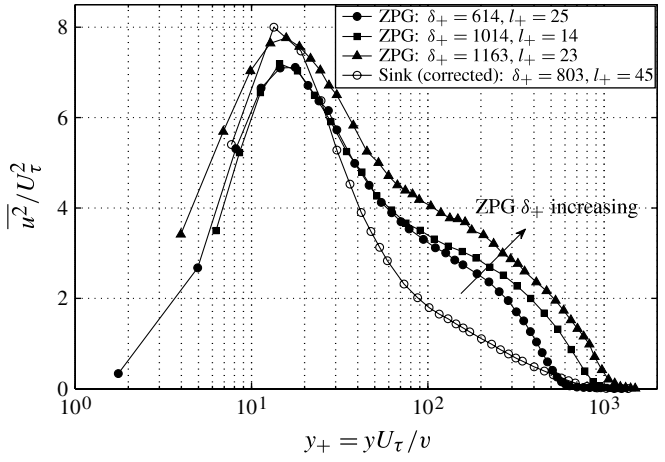


FIGURE 7. Comparison of wall-normal distributions of the streamwise intensity in three ZPG flows and the present sink flow. Sink flow profile is corrected for the spatial resolution ($l_+$) effect by employing the scheme of Smits *et al.* (2011); the profile beyond $y_+ = 100$ however has negligible $l_+$ effect. ZPG flows with $\delta_+ = 614$ and 1163 are our own measurements and that with $\delta_+ = 1014$ is from Hutchins & Marusic (2007*a*). Lines connecting the symbols are for visual aid only.

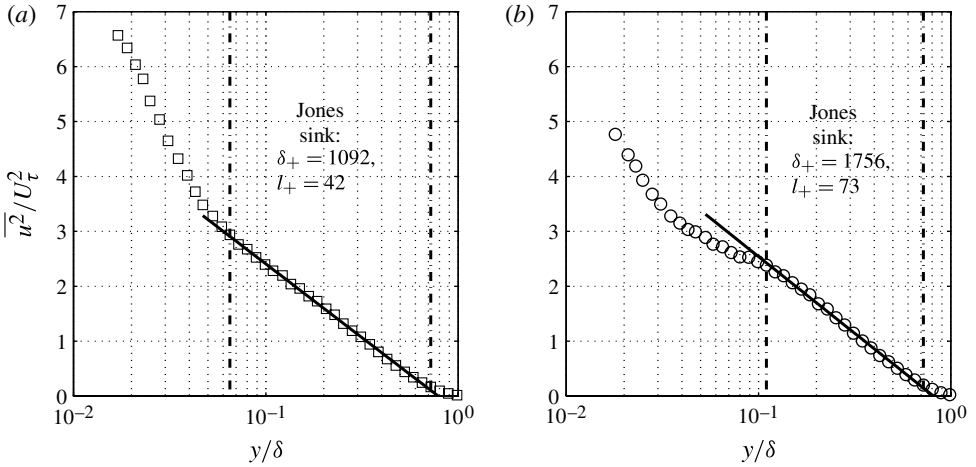


FIGURE 8. Wall-normal variations of the streamwise intensity in sink-flow TBLs of Jones (1998). The profiles are corrected for the spatial resolution ($l_+$) effect by employing the scheme of Smits *et al.* (2011); profiles beyond $y/\delta = 0.1$ have negligible $l_+$ effect. Solid lines indicate a logarithmic fit to the data between wall-normal positions marked by dashed-dotted vertical lines.

1756 from the study of Jones (1998). As may be noted, the overall trend of intensity variation in both plots is identical to that of figure 2(*a*). The profiles of figure 8 show distinct logarithmic variations of intensity over a considerable part of the boundary layer. None of the profiles indicate the presence of a strong bump or plateau in the intensity which is typical of ZPG flows. It therefore appears that the sink-flow FPG

suppresses the outer site just to the extent that the intensity varies logarithmically. Flow with $\delta_+ = 1756$ (figure 8*b*) shows a small bump in the intensity but this is perhaps due to the fact that this flow has not attained the asymptotic sink-flow state: the wake factor is still $\sim$0.1 and not zero as it is expected to be in an asymptotic sink-flow TBL (Jones 1998).

On the whole, the evidence presented above convincingly demonstrates that the steep (in general) and logarithmic (in particular, for sink flows) drop of intensity is not an artifact of the low Reynolds number but is distinctively an FPG effect.

## REFERENCES


DAVIDSON, P. A. & KROGSTAD, P. Å. 2009 A simple model for the streamwise fluctuations in the log-law region of a boundary layer. *Phys. Fluids* **21**, 055105.

DAVIDSON, P. A., NICKELS, T. B. & KROGSTAD, P. Å. 2006 The logarithmic structure function law in wall-layer turbulence. *J. Fluid Mech.* **550**, 51–60.

DIXIT, S. A. & RAMESH, O. N. 2008 Pressure-gradient-dependent logarithmic laws in sink flow turbulent boundary layers. *J. Fluid Mech.* **615**, 445–475.

DIXIT, S. A. & RAMESH, O. N. 2010 Large-scale structures in turbulent and reverse-transitional sink flow boundary layers. *J. Fluid Mech.* **649**, 233–273.

HARUN, Z., MONTY, J. P., MATHIS, R. & MARUSIC, I. 2013 Pressure gradient effects on the large-scale structure of turbulent boundary layers. *J. Fluid Mech.* **715**, 477–498.

HÖGSTRÖM, U., HUNT, J. C. R. & SMEDMAN, A. S. 2002 Theory and measurements for turbulence spectra and variances in the atmospheric neutral surface layer. *Boundary-Layer Meteorol.* **103**, 101–124.

HUTCHINS, N. & MARUSIC, I. 2007*a* Large-scale influences in near-wall turbulence. *Phil. Trans. R. Soc.* A **365**, 647–664.

HUTCHINS, N. & MARUSIC, I. 2007*b* Evidence of very long meandering features in the logarithmic region of turbulent boundary layers. *J. Fluid Mech.* **579**, 1–28.

HUTCHINS, N., NICKELS, T. B., MARUSIC, I. & CHONG, M. S. 2009 Hot-wire spatial resolution issues in wall-bounded turbulence. *J. Fluid Mech.* **635**, 103–136.

JONES, M. B. 1998 Evolution and structure of sink flow turbulent boundary layers. PhD thesis, University of Melbourne, Australia.

JONES, M. B., MARUSIC, I. & PERRY, A. E. 2001 Evolution and structure of sink-flow turbulent boundary layers. *J. Fluid Mech.* **428**, 1–27.

KATUL, G. & CHU, C. R. 1998 A theoretical and experimental investigation of energy-containing scales in the dynamic sublayer of boundary-layer flows. *Boundary-Layer Meteorol.* **86**, 279–312.

LAUREN, M. K., MENABDE, M., SEED, A. W. & AUSTIN, G. L. 1999 Characterisation and simulation of the multiscaling properties of the energy-containing scales of horizontal surface-layer winds. *Boundary-Layer Meteorol.* **90**, 21–46.

MARUSIC, I., MONTY, J. P., HULTMARK, M. & SMITS, A. J. 2013 On the logarithmic region in wall turbulence. *J. Fluid Mech.* **716**, R3.

METZGER, M., LYONS, A. & FIFE, P. 2008 Mean momentum balance in moderately favourable pressure gradient turbulent boundary layers. *J. Fluid Mech.* **617**, 107–140.

NICKELS, T. B., MARUSIC, I., HAFEZ, S. & CHONG, M. S. 2005 Evidence of the $k_1^{-1}$ law in a high-Reynolds-number turbulent boundary layer. *Phys. Rev. Lett.* **95**, 074501.

NICKELS, T. B., MARUSIC, I., HAFEZ, S., HUTCHINS, N. & CHONG, M. S. 2007 Some predictions of the attached eddy model for a high Reynolds number boundary layer. *Phil. Trans. R. Soc.* A **365**, 807–822.

NIKORA, V. 1999 Origin of the '$-1$' spectral law in wall-bounded turbulence. *Phys. Rev. Lett.* **83** (4), 734–736.

PERRY, A. E. & CHONG, M. S. 1982 On the mechanism of wall turbulence. *J. Fluid Mech.* **119**, 173–217.

PERRY, A. E., HENBEST, S. & CHONG, M. S. 1986 A theoretical and experimental study of wall turbulence. *J. Fluid Mech.* **165**, 163–199.

PERRY, A. E. & MARUSIC, I. 1995 A wall-wake model for the turbulence structure of boundary layers. Part 1. Extension of the attached eddy hypo thesis. *J. Fluid Mech.* **298**, 361–388.

SMITS, A. J., MONTY, J., HULTMARK, M., BAILEY, S. C. C., HUTCHINS, N. & MARUSIC, I. 2011 Spatial resolution correction for wall-bounded turbulence measurements. *J. Fluid Mech.* **676**, 41–53.

SREENIVASAN, K. R. 1989 The turbulent boundary layer. In *Frontiers in Experimental Fluid Mechanics* (ed. M. Gad-El-Hak), Springer.

TOWNSEND, A. A. 1976 *The Structure of Turbulent Shear Flow*, 2nd edn. Cambridge University Press.

UDDIN, A. K. M., PERRY, A. E. & MARUSIC, I. 1997 Application of the wavelet transform in turbulence. In *Second International Seminar on Fluid Mechanics and Heat Transfer, 17–18 December, Dhaka, Bangladesh*, pp. 25–34.

WEI, T., FIFE, P., KLEWICKI, J. & MCURTRY, P. 2005 Properties of the mean momentum balance in turbulent boundary layer, pipe and channel flows. *J. Fluid Mech.* **522**, 303–327.